J Med Ultrasonics (2016) 43:19–27
DOI 10.1007/s10396-015-0673-x

ORIGINAL ARTICLE

Enhancing effect of phase coherence factor for improvement of spatial resolution in ultrasonic imaging

Hideyuki Hasegawa[1]

Received: 21 July 2015 / Accepted: 3 September 2015 / Published online: 7 October 2015

Abstract
Purpose Spatial resolution is one of the important factors that determines ultrasound image quality. In the present study, methods using the phase variance of ultrasonic echoes received by individual transducer elements have been examined for improvement of spatial resolution.
Method An imaging method, i.e., phase coherence imaging, which uses the phase coherence factor (PCF) obtained from the phase variance of received ultrasonic echoes, was recently proposed. Spatial resolution is improved by weighting ultrasonic RF signals obtained by delay-and-sum (DAS) beam forming using PCF. In the present study, alternative PCFs, i.e., exponential PCF, harmonic PCF, and Gaussian PCF, have been proposed and examined for further improvement of spatial resolution.
Result Spatial resolutions realized by the proposed PCFs were evaluated by an experiment using a phantom. The full widths at half maxima of the lateral profiles of an echo from a string phantom were 2.61 mm (DAS only), 1.46 mm (conventional PCF), and 0.48–0.62 mm (proposed PCFs).
Conclusion The PCFs newly proposed in the present study showed better spatial resolutions than the conventional PCF. The proposed PCFs also realized better visualization of echoes from a diffuse scattering medium than the conventional PCF.

✉ Hideyuki Hasegawa
hasegawa@eng.u-toyama.ac.jp

[1] Graduate School of Science and Engineering for Research, University of Toyama, 3190 Gofuku, Toyama 930-8555, Japan

Keywords Phase variance · Coherence factor · Spatial resolution · Ultrasonic image

Introduction

Ultrasonography, which enables real-time and noninvasive imaging of the human body, is widely used in clinical situations. In the case of ultrasonography, spatial resolution is an important factor that determines image quality. Image and signal processing methods have been proposed to improve ultrasound image quality [1–5]. Development of an ultrasonic beam former is another strategy to improve image quality, and a number of studies on ultrasound beam forming have been conducted for improvement of the spatial resolution in ultrasonography.

Ultrasound beam forming using an array ultrasonic probe is required to obtain ultrasound images. The most common beam forming procedure is delay-and-sum (DAS) beam forming, which compensates for the differences among time delays of ultrasonic echoes received by individual transducer elements in an ultrasonic probe based on the geometrical information of each element and the receiving focal point.

Recently, adaptive beam forming has been studied intensively [6–12]. This method improves the spatial resolution significantly by adaptively determining the weights to individual echoes in the DAS beam forming procedure. Although adaptive beam forming provides excellent performance, its high computational cost is a barrier to implementation in commercial ultrasound scanners.

Methods that utilize the coherence among echoes received by individual transducer elements have also been proposed for improvement of the spatial resolution. Such methods use the coherence factor [13, 14] or autocorrelation

function of element echo signals [15, 16] to suppress undesired echoes, which come from spatial points other than the receiving focal point. Camacho et al. have proposed the phase coherence factor (PCF), which evaluates the coherency of element echo signals using their phase variance, to suppress undesirable echoes [17]. They have also examined how to control the effect of PCF. However, they have concentrated on how to weaken the effect of PCF and have not extensively examined how to enhance the effect of PCF. The reason for this may be because PCF suppresses echoes from a diffuse scattering medium and such echoes would be further suppressed if the effect of PCF was enhanced. In our previous study [18], it was shown that suppression of echoes from a diffuse scattering medium could be avoided by estimating PCF with sub-aperture beam forming. Using sub-aperture beam forming, it would be possible to further enhance the effect of PCF (improvement of spatial resolution) without significant suppression of echoes from a diffuse scattering medium. In the present study, some strategies have been proposed to further enhance the effect of PCF, and the performances of the proposed methods have been examined through a basic experiment using a phantom.

Materials and methods

Phase coherence factor (PCF)

The phase coherence factor (PCF) [17] is obtained using the phase variance of ultrasonic echoes received by individual transducer elements of an ultrasonic probe. The phase standard deviation σ is estimated after delay compensation done by a conventional DAS beam former. As illustrated in Fig. 1a, after delay compensation, there is no phase variance among the element echo signals when the echo is coming from the receiving focal point. On the other hand, as illustrated in Fig. 2b, c, the phase variance increases when the echo is coming from a spatial point other than the focal point. Using the phase standard deviation σ, PCF is expressed as follows:

$$\mathrm{PCF} = 1 - \gamma \frac{\sigma}{\sigma_0}, \tag{1}$$

where γ $(0 \leq \gamma \leq 1)$ is the control parameter and σ_0 is the nominal standard deviation of $\pi/3^{0.5}$ of a uniform distribution between $-\pi$ and π [17]. In the case of the conventional phase coherence imaging proposed in [17], the phase standard deviation σ is estimated using echoes received by individual elements.

By weighting beamformed RF signals obtained with a conventional DAS beam former by PCF, undesired echoes, which come from spatial points other than the receiving focal point, are suppressed. In [17], the control parameter γ was proposed to weaken the effect of PCF (γ of less than 1 weakens the effect of PCF). In the present study, γ was set at 1.

Enhancement of the effect of PCF

In the present study, three kinds of PCFs have been examined for enhancement of the effect of PCF. For estimation of the enhanced PCFs proposed here, the phase standard deviation σ was obtained using the outputs of sub-aperture beam formers [18] for visualization of echoes from a diffuse scattering medium.

Exponential PCF

In [17], the parameter γ $(0 \leq \gamma \leq 1)$ was introduced to weaken the effect of PCF. In the present study, the

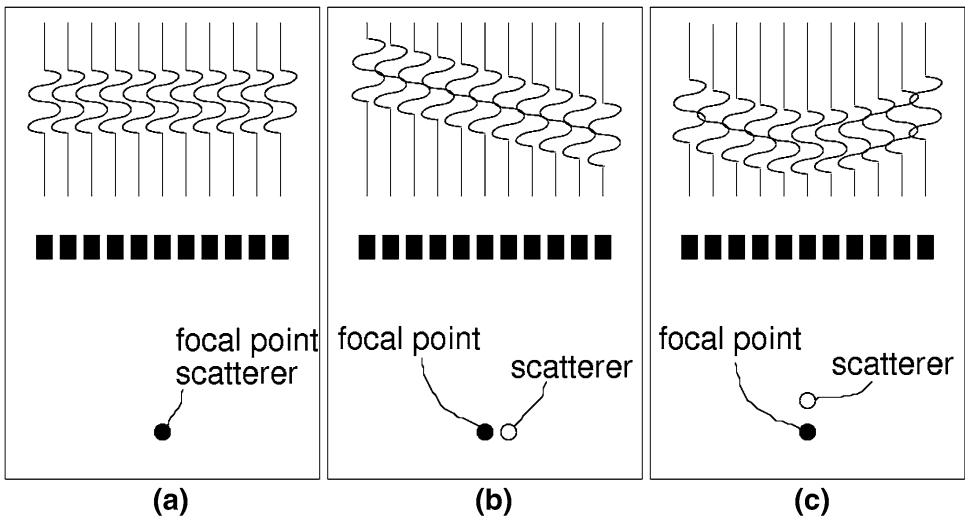

Fig. 1 Illustration of delay compensation in DAS beam former with **a** no focusing error and **b**, **c** slight focusing errors

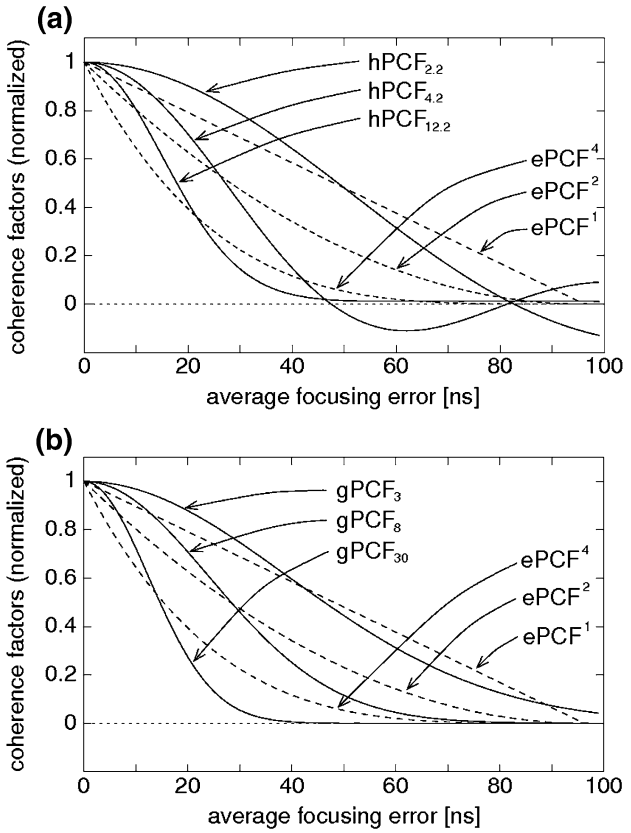

Fig. 2 Phase coherence factors plotted as functions of average focusing error τ_e. **a** Exponential PCF ($ePCF^{\alpha}$) and harmonic PCF ($hPCF_{\beta}$). **b** Exponential PCF ($ePCF^{\alpha}$) and Gaussian PCF ($gPCF_{\rho}$)

exponential PCF, $ePCF^{\alpha} = PCF^{\alpha}$, was examined to enhance the effect of PCF. The concept of the exponential coherence factor has already been proposed in [17] for the sign coherence factor, but it was also used to weaken ($\alpha \leq 1$) the effect of the coherence factor in [17]. In the present study, α of 1, 2, and 4 were examined to enhance the effect of PCF.

Harmonic PCF

The phase standard deviation σ used in PCF corresponds to average focusing error τ_e (s), and thus, σ can be considered to be the phase standard deviation at ultrasonic center frequency f_0 owing to the focusing error τ_e. In the present study, the phase standard deviation was modeled as $\sigma = 2\pi f_0 \tau_e$. By considering phase standard deviations $\beta\sigma$ at frequencies higher than f_0 ($\beta > 1$), undesired echoes are expected to be more suppressed than using σ at a single frequency of f_0. In the present study, the harmonic PCF, $hPCF_{\beta}$, is proposed as follows:

$$hPCF_{\beta} = \sum_{x} w_x \times \cos(x \times \sigma), \tag{2}$$

$$w_x = \exp\left\{-a \times \frac{(xf_0)^2}{f_0^2}\right\}, \tag{3}$$

where $0 \leq x \leq \beta$. The Gaussian weight w_x was applied to the harmonic component $\cos(x \times \sigma)$ to reduce the effect of the use of a finite range of β.

In Fig. 2a, exponential PCF $ePCF^{\alpha}$ and harmonic PCF $hPCF_{\beta}$ are plotted as functions of average focusing error τ_e. To realize similar widths at half maxima to those obtained by $ePCF^{\alpha}$ at $\alpha = 1,\ 2,$ and 4, β of 2.2, 4.2, and 12.2 were examined. The parameter a is an empirical parameter, and in the present study, its value was set at 0.04 to obtain similar widths at half maxima of $ePCF^{\alpha}$ and $hPCF_{\beta}$. As shown in Fig. 2a, side lobes are found at β of 2.2 and 4.2, and a higher value of β is required to reduce the side lobe level.

Gaussian PCF

To suppress the side lobes of the harmonic PCF shown in Fig. 2a, Gaussian PCF $gPCF_{\rho}$ was also proposed in the present study as follows:

$$gPCF_{\rho} = \exp\left\{-\rho \times \left(\frac{\sigma}{\sigma_0}\right)^2\right\}. \tag{4}$$

In Fig. 2b, exponential PCF $ePCF^{\alpha}$ and Gaussian PCF $gPCF_{\rho}$ are plotted as functions of average focusing error τ_e. To realize similar widths at half maxima to those of $ePCF^{\alpha}$ at $\alpha = 1,\ 2,$ and 4, ρ of 3, 8, and 30 were examined in the present study. As shown in Fig. 2b, $ePCF^{\alpha}$ shows a steep decay around an average focusing error of 0 but shows a slower decay at larger average focusing errors. On the other hand, Gaussian PCF $gPCF_{\rho}$ shows a faster decay than exponential PCF $ePCF^{\alpha}$ (corresponds to lower side lobe level).

Experimental setup

An ultrasound imaging phantom (model 040GSE, CIRS Inc., Norfolk, VA, USA) was used for evaluation of the improvement in imaging spatial resolution. A phased array ultrasonic probe at a nominal center frequency of 3.75 MHz (PU-0541, Ueda Japan Radio, Ueda, Japan) was used, and ultrasonic echo signals received by individual transducer elements were acquired by a custom-made ultrasound scanner (RSYS0002, Microsonic, Tokyo, Japan) at a sampling frequency of 31.25 MHz. The beamforming procedure was performed off-line on the ultrasonic echo

signals received by the individual elements. The element pitch of the phased array was 0.2 mm.

In the present study, a diverging transmit beam [19] from a virtual point source was produced using 96 active elements. The virtual point source was placed at 30 mm behind the array. An ultrasonic image was created by only one transmission of the diverging beam [20, 21].

Experimental results

Figure 3 shows B-mode images of the phantom. Figure 3a was obtained by DAS beam forming without PCF. Figure 3b–d shows B-mode images obtained with exponential PCFs $ePCF^1$, $ePCF^2$, and $ePCF^4$, respectively, without sub-aperture beam forming. In Fig. 3b–d, the spatial resolution is improved by increasing coefficient α. However, echoes from a diffuse scattering medium are suppressed significantly, and the estimation of PCF without sub-aperture beam forming (conventional way to estimate PCF) [17] is not suitable for enhancing the effect of PCF.

B-mode images in Fig. 3e–m were obtained with 3-sub-aperture beam forming [18]. Each sub-aperture was composed of 32 elements. Figure 3e–g shows B-mode images obtained with exponential PCFs $ePCF^1$, $ePCF^2$, and $ePCF^4$, respectively; Fig. 3h–j was obtained with harmonic PCFs $hPCF_{2.2}$, $hPCF_{4.2}$, and $hPCF_{12.2}$, respectively; and Fig. 3k–m were obtained with Gaussian PCFs $gPCF_3$, $gPCF_8$, and $gPCF_{30}$, respectively. As can be seen in those figures, the estimation of PCF with sub-aperture beam forming realizes improvement of the spatial resolution and visualization of echoes from a diffuse scattering medium simultaneously [18]. Also, the diffuse scattering medium was visualized even when the effect of PCF was enhanced (at larger values of α, β, and ρ).

Figure 4 shows lateral echo amplitude profiles obtained at a range distance of 42.4 mm. A large echo at a lateral angle of $-1.9°$ is an echo from a string. As shown in Fig. 4, PCFs with sub-aperture beam forming realizes better visualization of echoes from a diffuse scattering medium than PCFs without sub-aperture beam forming. Also, similar peak levels of echoes from a diffuse scattering medium obtained by ePCF, hPCF, and gPCF show that they have similar ability to visualize echoes from a diffuse scattering medium.

The lateral spatial resolution was evaluated by estimating the full width at half maximum of the echo from the string located at a lateral angle of $-1.9°$ in Fig. 4. The results are summarized in Table 1. For each PCF, the spatial resolution was significantly improved by increasing the coefficients α, β, or ρ. However, as mentioned above, ePCF without sub-aperture beam forming significantly suppressed echoes from a diffuse scattering medium by increasing α , and thus, it is not suitable for enhancing the effect of PCF. When we look at side lobes around the echo from the string, gPCF achieved the lowest side lobe level, as expected from Fig. 2.

Figure 5 shows axial echo amplitude profiles at a lateral position of $-1.9°$ obtained by the respective methods. The axial full width at half maxima was also obtained from an echo from a string at a range distance of 42.4 mm, and is summarized in Table 2. The range spatial resolutions obtained with PCFs were better than those obtained by DAS only. Exponential PCF $ePCF^{\alpha}$ without sub-aperture beam forming realized a better range resolution than PCFs with sub-aperture beam forming.

Discussion

In the present study, methods for enhancement of the effect of PCF were examined. In the case of conventional phase coherence imaging without sub-aperture beam forming [17], it is difficult to enhance the effect of PCF because echoes from diffuse scattering media are suppressed significantly. By estimating PCF with sub-aperture beam forming, improvement of the spatial resolution and visualization of echoes from a diffuse scattering medium could be realized simultaneously. In the present study, three kinds of PCFs, i.e., $ePCF^{\alpha}$, $hPCF_{\beta}$, and $gPCF_{\rho}$, were examined for further enhancement of the effect of PCF. These three PCFs showed similar levels of spatial resolution and visualization of echoes from a diffuse scattering medium, but $gPCF_{\rho}$ showed a lower side lobe level. Therefore, $gPCF_{\rho}$ is preferable among the proposed enhanced PCFs.

In principle, PCF more greatly suppresses echoes with larger phase variances. The phase variance includes phase fluctuations owing to focusing error, interference among echoes, and electrical noise. Suppression of echoes with focusing errors is a desirable effect. On the other hand, suppression of echoes from a focal point due to interference among echoes and electrical noise are undesirable effects. The effect of interference among echoes can be reduced by suppressing echoes from spatial points other than the focal point using sub-aperture beam forming [18], and thus, echoes from a diffuse scattering medium (containing a lot of scatterers) can be better visualized by PCF with sub-aperture beam forming than PCF without sub-aperture beam forming. However, echoes from spatial points other than the focal point cannot be suppressed perfectly due to the finite size of each sub-aperture. Therefore, the estimated phase variance includes the residual effects of interference and noise. An echo with a

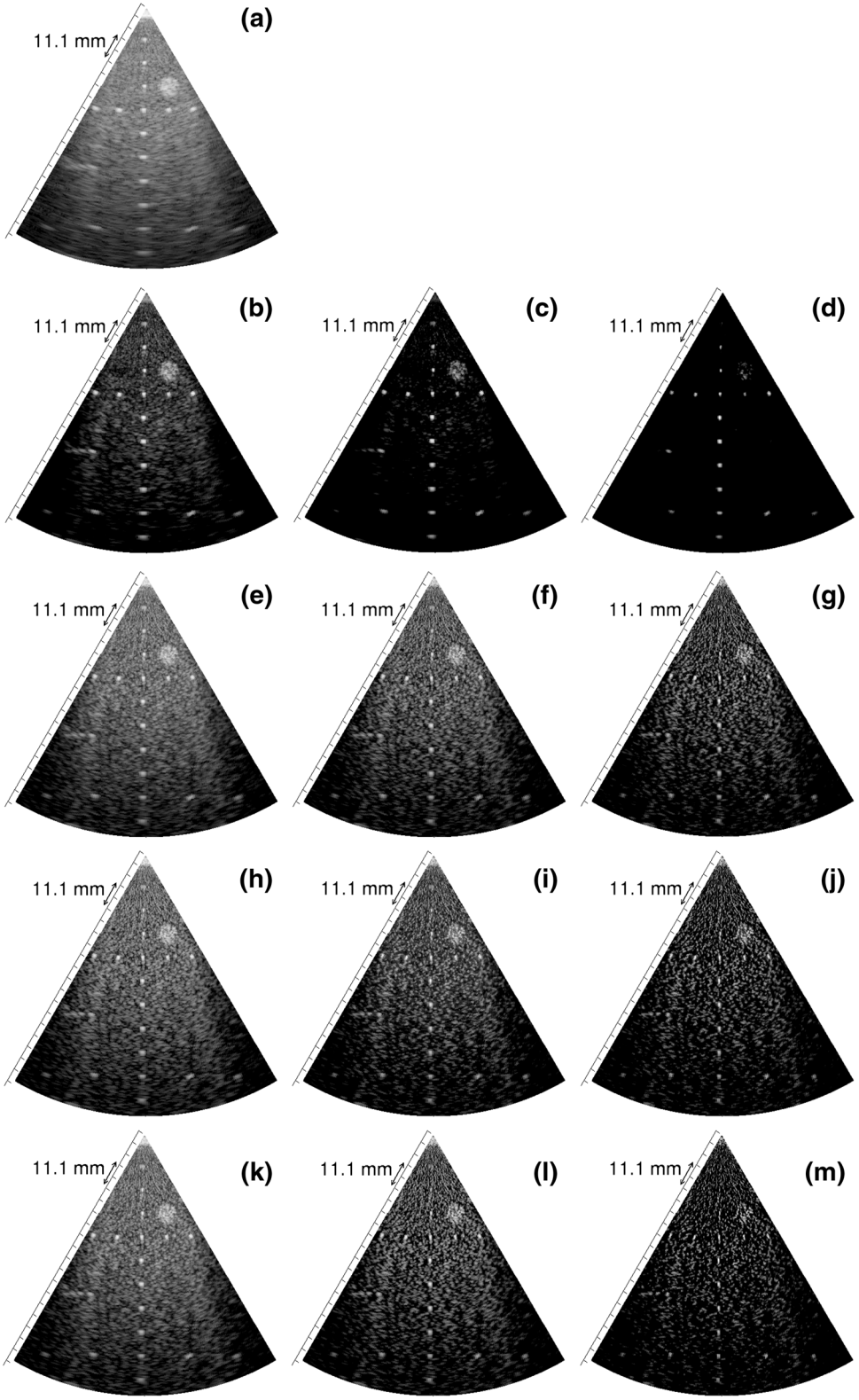

Fig. 3 B-mode images of phantom. **a** DAS beam forming without PCF. **b** Exponential PCF ePCF[1] without sub-aperture beam forming. **c** Exponential PCF ePCF[2] without sub-aperture beam forming. **d** Exponential PCF ePCF[4] without sub-aperture beam forming. **e** Exponential PCF ePCF[1] with three sub-apertures. **f** Exponential PCF ePCF[2] with three sub-apertures. **g** Exponential PCF ePCF[4] with three sub-apertures. **h** Harmonic PCF $hPCF_{2.2}$ with three sub-apertures. **i** Harmonic PCF $hPCF_{4.2}$ with three sub-apertures. **j** Harmonic PCF $hPCF_{12.2}$ with three sub-apertures. **k** Gaussian PCF $gPCF_3$ with three sub-apertures. **l** Gaussian PCF $gPCF_8$ with three sub-apertures. **m** Gaussian PCF $gPCF_{30}$ with three sub-apertures

lower amplitude is more influenced by interference from other echoes, and also, electrical noise more greatly influences an echo with a lower amplitude. Such influences increase the phase variance. Therefore, echoes with lower amplitudes tend to be suppressed when the effect of PCF is enhanced. Such a phenomenon is observed in the results

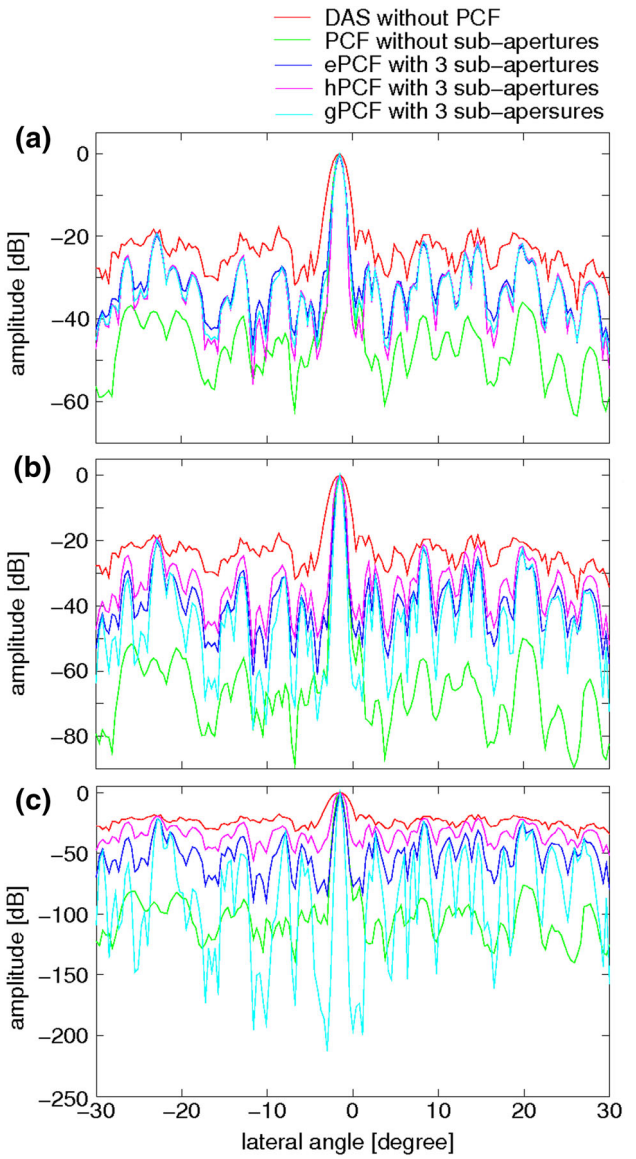

Fig. 4 Lateral amplitude profiles at a range distance of 42.4 mm. **a** DAS without PCF, $ePCF^1$ without sub-aperture beam forming, $ePCF^1$, $hPCF_{2.2}$, and $gPCF_3$ with three sub-apertures. **b** DAS without PCF, $ePCF^2$ without sub-aperture beam forming, $ePCF^2$, $hPCF_{4.2}$, and $gPCF_8$ with three sub-apertures. **c** DAS without PCF, $ePCF^4$ without sub-aperture beam forming, $ePCF^4$, $hPCF_{12.2}$, and $gPCF_{30}$ with three sub-apertures

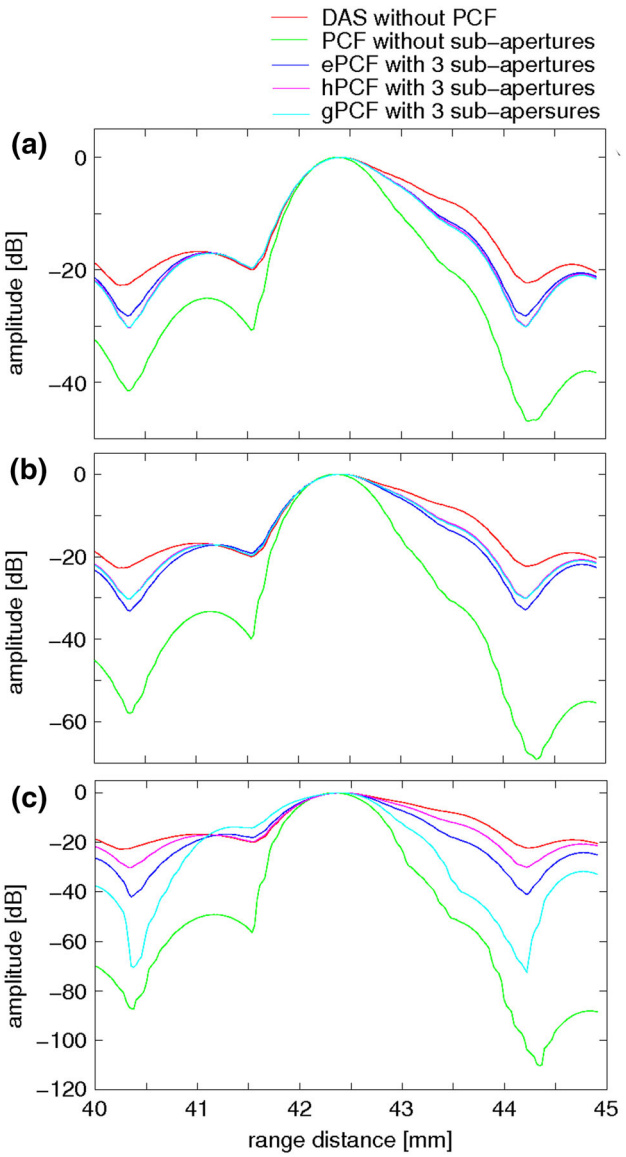

Fig. 5 Axial amplitude profiles at a lateral position of −1.9°. **a** DAS without PCF, $ePCF^1$ without sub-aperture beam forming, $ePCF^1$, $hPCF_{2.2}$, and $gPCF_3$ with three sub-apertures. **b** DAS without PCF, $ePCF^2$ without sub-aperture beam forming, $ePCF^2$, $hPCF_{4.2}$, and $gPCF_8$ with three sub-apertures. **c** DAS without PCF, $ePCF^4$ without sub-aperture beam forming, $ePCF^4$, $hPCF_{12.2}$, and $gPCF_{30}$ with three sub-apertures

Table 1 Lateral full widths at half maxima obtained by respective methods

DAS w/o sub-apertures	2.61 mm				
$ePCF^1$ w/o sub-apertures	1.46 mm	$ePCF^2$ w/o sub-apertures	1.14 mm	$ePCF^4$ w/o sub-apertures	0.84 mm
$ePCF^1$ w/3 sub-apertures	1.37 mm	$ePCF^2$ w/3 sub-apertures	0.93 mm	$ePCF^4$ w/3 sub-apertures	0.62 mm
$hPCF_{2.2}$ w/3 sub-apertures	1.41 mm	$hPCF_{4.2}$ w/3 sub-apertures	0.87 mm	$hPCF_{12.2}$ w/3 sub-apertures	0.55 mm
$gPCF_3$ w/3 sub-apertures	1.36 mm	$gPCF_8$ w/3 sub-apertures	0.91 mm	$gPCF_{30}$ w/3 sub-apertures	0.48 mm

Table 2 Axial full widths at half maxima obtained by respective methods

DAS w/o sub-apertures	1.29 mm				
$ePCF^{1}$ w/o sub-apertures	0.85 mm	$ePCF^{2}$ w/o sub-apertures	0.77 mm	$ePCF^{4}$ w/o sub-apertures	0.73 mm
$ePCF^{1}$ w/3 sub-apertures	1.13 mm	$ePCF^{2}$ w/3 sub-apertures	1.08 mm	$ePCF^{4}$ w/3 sub-apertures	1.00 mm
$hPCF_{2.2}$ w/3 sub-apertures	1.13 mm	$hPCF_{4.2}$ w/3 sub-apertures	1.00 mm	$hPCF_{12.2}$ w/3 sub-apertures	0.95 mm
$gPCF_{3}$ w/3 sub-apertures	1.12 mm	$gPCF_{8}$ w/3 sub-apertures	1.02 mm	$gPCF_{30}$ w/3 sub-apertures	0.98 mm

shown in Fig. 3. In Fig. 3a, the circular hyperechoic region in the phantom contains a region with echo amplitudes similar to those of a diffuse scattering medium along its edge around the 10 o'clock direction. By enhancing the effect of PCF, the difference in the amplitude levels between the dominant echoes, such as an echo from a string, and the weaker echo from a diffuse scattering medium is increased, as shown in Fig. 4. Therefore, amplitude differences between strong echoes and weaker echoes in the circular hyperechoic region are increased by enhancing the effect of PCF, as shown in Fig. 3g, j, m. Also, the point spread function is significantly sharpened by the enhanced PCF. As a result, the shape of the circular hyperechoic region is slightly changed. Therefore, it may be better to control the effect of PCF depending on the situation. For example, to observe the overall shape of an organ, such as the liver, it may be better not to enhance the effect of PCF so much. On the other hand, to observe highly coherent echoes from structures or inclusions in an organ, such as fibrotic nodules in the liver and micro bubbles in vessels, with a high spatial resolution, it would be beneficial to enhance the effect of PCF. The proposed method is useful because the effect of PCF can be controlled easily by adjusting the parameters α, β, and ρ.

Even though the effects of PCF are controllable, the relationship between suppression of echoes and phase fluctuation owing to the interference among echoes and noise should be elucidated quantitatively. Also, if we consider optimization of the proposed methods, the optimization needs to be performed under various conditions of the structure of a target (whether target structure produces strong echoes or not), echo signal-to-noise ratios, and so forth. Such issues will be investigated in future work.

Evaluation of spatial resolution revealed that PCFs with sub-aperture beam forming yielded better lateral spatial resolutions than PCFs without sub-aperture beam forming. On the other hand, PCFs without sub-aperture beam forming yielded a better axial spatial resolution than PCFs with sub-aperture beam forming.

The phase standard deviation σ of echoes received by individual elements can be said to contain the phase standard deviation σ_{int} induced by interference between echoes and σ_{fe} induced by focusing error. The phase standard deviation σ estimated with sub-aperture beam forming contains less phase standard deviation σ_{int} induced by interference because echoes from spatial points other than the receiving focal point are suppressed by sub-aperture beam forming. The effect of the phase standard deviation σ_{int} induced by interference can be considered to be similar both in the lateral and axial directions. Therefore, let us consider the phase standard deviations σ_{fe} induced by focusing errors in the lateral and axial directions. In the present study, the lateral and axial full widths at half maxima were about 2.6 and 1.3 mm, respectively. So, let us evaluate theoretically the phase standard deviations σ_{fe} at lateral and axial focusing errors corresponding to 1.3 and 0.65 mm (distances of the points at half maxima from the peak) at an ultrasonic center frequency of 3 MHz. The evaluated phase standard deviations σ_{fe} at the respective focusing errors were 1.09 rad. (lateral) and 0.06 rad. (axial) at an element pitch of 0.2 mm and number of active elements of 96. Sub-aperture beam forming suppresses the effect of interference, and the residual phase variance σ_{fe} owing to focusing error is larger in the lateral direction than in the axial direction. Therefore, PCFs with sub-aperture beam forming are thought to improve the lateral spatial resolution but degrade the axial spatial resolution compared to PCFs without sub-aperture beam forming. In terms of the axial spatial resolution, a conventional PCF without sub-aperture beam forming showed better performance. However, it is difficult to use it for general-purpose imaging, in which diffuse scattering media should also be visualized. A conventional PCF without sub-aperture beam forming might be useful for extraction of only strong echoes. PCFs with sub-aperture beam forming would be more suitable for general-purpose imaging and can extract highly coherent echoes even in a diffuse scattering medium when the effect of PCF is enhanced by the proposed method.

In the present study, detailed analyses have not been done with respect to $hPCF_{\beta}$ and $gPCF_{\rho}$ without sub-aperture beam forming because they also degrade imaging of diffuse scattering media as in the case of a conventional PCF without sub-aperture beam forming. Figure 6 shows B-mode images obtained by $hPCF_{\beta}$ and $gPCF_{\rho}$ without sub-aperture beam forming. As can be seen in Fig. 6, echoes from a diffuse scattering medium are significantly suppressed by $hPCF_{\beta}$ and $gPCF_{\rho}$ without sub-aperture

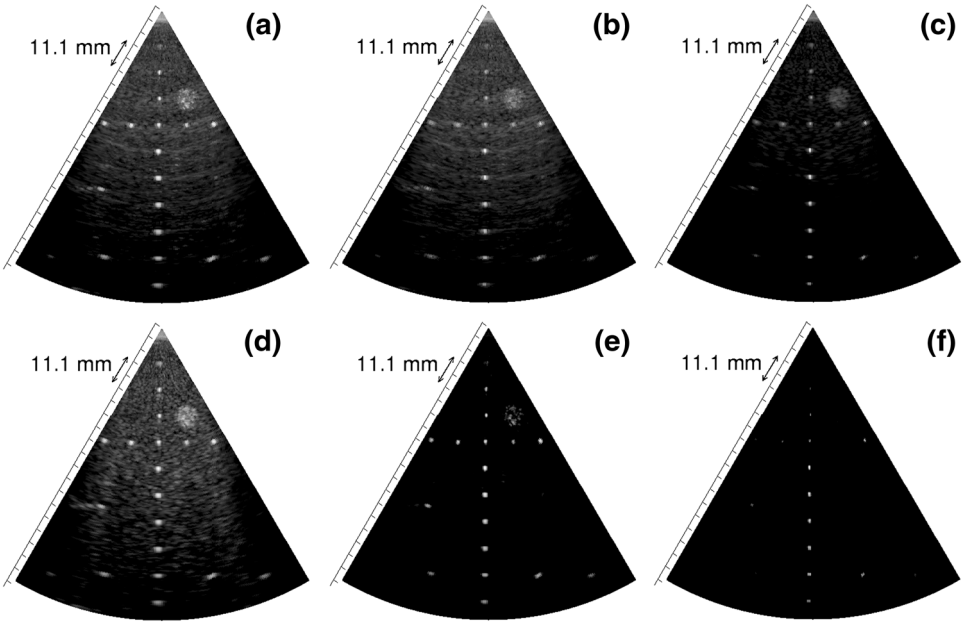

Fig. 6 B-mode images of phantom obtained without sub-aperture beam forming.
a Harmonic PCF $hPCF_{2.2}$.
b Harmonic PCF $hPCF_{4.2}$.
c Harmonic PCF $hPCF_{12.2}$.
d Gaussian PCF $gPCF_3$.
e Gaussian PCF $gPCF_8$.
f Gaussian PCF $gPCF_{30}$

beam forming. Echoes from a diffuse scattering medium in B-mode images obtained with $hPCF_\beta$ are slightly more visible owing to higher side lobes in $hPCF_\beta$ than $gPCF_\rho$, as shown in Fig. 2. However, sub-aperture beam forming is also necessary for $hPCF_\beta$ and $gPCF_\rho$ to realize further improvement in spatial resolution without significant suppression of echoes from the diffuse scattering medium.

Also, phase coherence imaging with sub-aperture beam forming reduces computational load significantly. Conventional phase coherence imaging without sub-aperture beam forming requires the estimation of phases of echoes received by individual elements (96 elements in the present study). Phase coherence imaging with sub-aperture beam forming requires the phase estimation on outputs from sub-apertures (only three sub-apertures in the present study). It would be preferable for real-time imaging.

Conclusions

PCF is effective for improving the spatial resolution in ultrasonic imaging. However, a conventional PCF estimated without sub-aperture beam forming suppresses echoes from a diffuse scattering medium significantly. Therefore, it is not suitable for general-purpose imaging to further enhance the effect of a conventional PCF. In the present study, PCF was estimated with sub-aperture beam forming to visualize echoes from a diffuse scattering medium, and methods for enhancement of the effect of PCF were examined. The proposed PCFs realized a further improvement in the spatial resolution and visualization of echoes from a diffuse scattering medium simultaneously. The proposed PCFs are more computationally effective than the conventional PCF, and it would be suitable for real-time imaging.

Acknowledgments This study was supported by JSPS KAKENHI Grant Number 26289123.

Compliance with ethical standards

Ethical considerations Animal and human subjects were not used in this study.

Conflict of interest None.

References

1. Iraca D, Landini L, Verrazzani L. Power spectrum equalization for ultrasonic image restoration. IEEE Trans Ultrason Ferroelectr Freq Control. 1989;36:216–22.
2. Taxt T, Jirik R. Superresolution of ultrasound images using the first and second harmonic signal. IEEE Trans Ultrason Ferroelectr Freq Control. 2004;51:163–75.
3. Yeoh WS, Zhang C. Constrained least squares filtering algorithm for ultrasound image deconvolution. IEEE Trans Biomed Eng. 2006;53:2001–7.
4. Kageyama S, Hasegawa H, Kanai H. Increasing bandwidth of ultrasound radio frequency echoes using Wiener filter for improvement of accuracy in measurement of intima-media thickness. Jpn J Appl Phys. 2013;52:07HF04-1-7.
5. Taki H, Taki K, Sakamoto T, et al. High range resolution ultrasonographic vascular imaging using frequency domain interferometry with the capon method. IEEE Trans Med Imaging. 2012;31:417–29.
6. Capon J. High-resolution frequency-wavenumber spectrum analysis. Proc IEEE. 1969;57:1408–18.
7. Synnevåg JF, Austeng A, Holm S. Adaptive beam forming applied to medical ultrasound imaging. IEEE Trans Ultrason Ferroelectr Freq Control. 2007;54:1606–13.

8. Holfort IK, Gran F, Jensen JA. Broadband minimum variance beam forming for ultrasound imaging. IEEE Trans Ultrason Ferroelectr Freq Control. 2009;56:314–25.
9. Synnevåg JF, Austeng A, Holm S. Benefits of minimum variance beam forming in medical ultrasound imaging. IEEE Trans Ultrason Ferroelectr Freq Control. 2009;56:1868–79.
10. Blomberg AEA, Holfort IK, Austeng A, et al. APES beam forming applied to medical ultrasound imaging. IEEE Int Ultrason Symp Proc. 2009;2009:2347–50.
11. Åsen JP, Buskenes JI, Nilsen CIC, et al. Implementing Capon beam forming on a GPU for real-time cardiac ultrasound imaging. IEEE Trans Ultrason Ferroelectr Freq Control. 2014;61:76–85.
12. Hasegawa H, Kanai H. Effect of element directivity on adaptive beam forming applied to high-frame-rate ultrasound. IEEE Trans Ultrason Ferroelectr Freq Control. 2015;62:511–23.
13. Li P, Li M. Adaptive imaging using the generalized coherence factor. IEEE Trans Ultrason Ferroelectr Freq Control. 2003;50:128–41.
14. Wang SL, Chang CH, Yang HC, et al. Performance evaluation of coherence-based adaptive imaging using clinical breast data. IEEE Trans Ultrason Ferroelectr Freq Control. 2007;54:1669–79.
15. Dahl JJ, Hyun D, Lediju M, et al. Lesion detectability in diagnostic ultrasound with short-lag spatial coherence imaging. Ultrason Imaging. 2011;33:119–33.
16. Lediju Bell MA, Goswami R, Kisslo JA, et al. Short-lag spatial coherence imaging of cardiac ultrasound data: initial clinical results. Ultrasound Med Biol. 2013;39:1861–74.
17. Camacho J, Parrilla M, Fritsch C. Phase coherence imaging. IEEE Trans Ultrason Ferroelectr Freq Control. 2009;56:958–74.
18. Hasegawa H, Kanai H. Effect of sub-aperture beam forming on phase coherence imaging. IEEE Trans Ultrason Ferroelectr Freq Control. 2014;61:1779–90.
19. Hasegawa H, Kanai H. High-frame-rate echocardiography using diverging transmit beams and parallel receive beam forming. J Med Ultrason. 2011;38:129–40.
20. Takahashi H, Hasegawa H, Kanai H. Echo speckle imaging of blood particles with high-frame-rate echocardiography. Jpn J Appl Phys. 2014;53:07KF08-1-7.
21. Takahashi H, Hasegawa H, Kanai H. Echo motion imaging with adaptive clutter filter for assessment of cardiac blood flow. Jpn J Appl Phys. 2015;54:07HF09-1-8.